Optical measurements of the laser-induced ultrasonic waves on moving objects

Tomaž Požar,* Peter Gregorčič, and Janez Možina

Faculty of Mechanical Engineering, University of Ljubljana, Aškerčeva 6, 1000 Ljubljana, Slovenia
**tomaz.pozar@fs.uni-lj.si*

Abstract: We performed a single-shot, contactless measurement of ultrasonic waves on a laser-propelled rod with a homodyne quadrature laser interferometer (HQLI) during the entire duration of its motion. This is the first such experimental demonstration of the laser-induced motion of an elastic body where the most important mechanisms that reveal the nature of its motion are presented and explained. Furthermore, these measurements quantitatively demonstrate that the HQLI is an appropriate tool for monitoring high-amplitude (1.3 μm) and high-frequency (200 MHz) ultrasonic waves on moving objects. The applicability of the HQLI can also be extended to measure other optodynamic and high-frequency transient phenomena with a constant sensitivity and a resolution below 1 nm.

OCIS codes: (040.0040) Detectors; (120.0120) Instrumentation, measurement, and metrology; (120.3180) Interferometry; (350.3390) Laser materials processing; (350.5500) Propagation; (350.7420) Waves.

References and links

1. C. B. Scruby, and L. E. Drain, *Laser Ultrasonics: Techniques and Applications* (Adam Hilger, Bristol, 1990).
2. J. P. Monchalin, "Optical-Detection of Ultrasound," IEEE T. Ultrason. Ferr. **33**(5), 485–499 (1986).
3. S. J. Davies, C. Edwards, G. S. Taylor, and S. B. Palmer, "Laser-Generated Ultrasound: Its Properties, Mechanisms and Multifarious Applications," J. Phys. D Appl. Phys. **26**(3), 329–348 (1993).
4. R. J. Dewhurst, and Q. Shan, "Optical remote measurement of ultrasound," Meas. Sci. Technol. **10**(11), 201 (1999).
5. T. Požar, and J. Možina, "Optodynamic description of a linear momentum transfer from a laser induced ultrasonic wave to a rod," Appl. Phys., A Mater. Sci. Process. **91**(2), 315–318 (2008).
6. P. Gregorčič, R. Petkovšek, and J. Možina, "Investigation of a cavitation bubble between a rigid boundary and a free surface," J. Appl. Phys. **102**(9), 094904 (2007).
7. R. Petkovšek, A. Babnik, and J. Diaci, "Optodynamic monitoring of the laser drilling of through-holes in glass ampoules," Meas. Sci. Technol. **17**(10), 2828–2834 (2006).
8. T. Požar, R. Petkovšek, and J. Možina, "Dispersion of an optodynamic wave during its multiple transitions in a rod," Appl. Phys. Lett. **92**(23), 234101–234103 (2008).
9. B. Hu, and W. Schiehlen, "Multi-time scale simulation for impact systems: from wave propagation to rigid-body motion," Arch. Appl. Mech. **72**, 885–898 (2003).
10. T. Požar, and J. Možina, ""Homodyne Quadrature Laser Interferometer Applied for the Studies of Optodynamic Wave Propagation in a Rod," Stroj. Vestn. –," J. Mech. Eng. **55**, 575–580 (2009).
11. N. Bobroff, "Recent advances in displacement measuring interferometry," Meas. Sci. Technol. **4**(9), 907–926 (1993).
12. P. Gregorčič, T. Požar, and J. Možina, "Quadrature phase-shift error analysis using a homodyne laser interferometer," Opt. Express **17**(18), 16322–16331 (2009).
13. S. Strgar, and J. Možina, ""An optodynamic determination of the depth of laser-drilled holes by the simultaneous detection of ultrasonic waves in the air and in the workpiece," Ultrasonics **40**(1-8), 791–795 (2002).
14. A. S. Ergun, A. Atalar, B. Temelkuran, and E. Ozbay, "A sensitive detection method for capacitive ultrasonic transducers," Appl. Phys. Lett. **72**(23), 2957–2959 (1998).
15. A. S. Murfin, R. A. J. Soden, D. Hatrick, and R. J. Dewhurst, "Laser-ultrasound detection systems: a comparative study with Rayleigh waves," Meas. Sci. Technol. **11**(8), 1208–1219 (2000).
16. T. Yabe, C. Phipps, M. Yamaguchi, R. Nakagawa, K. Aoki, H. Mine, Y. Ogata, C. Baasandash, M. Nakagawa, E. Fujiwara, K. Yoshida, A. Nishiguchi, and I. Kajiwara, "Microairplane propelled by laser driven exotic target," Appl. Phys. Lett. **80**(23), 4318–4320 (2002).
17. B. Hu, W. Schiehlen, and P. Eberhard, "Comparison of analytical and experimental results for longitudinal impacts on elastic rods," J. Vib. Control **9**, 157–174 (2003).
18. K. Anju, K. Sawada, A. Sasoh, K. Mori, and E. Zaretsky, "Time-resolved measurements of impulse generation in pulsed laser-ablative propulsion," J. Propul. Power **24**(2), 322–329 (2008).

#119489 - $15.00 USD Received 3 Nov 2009; accepted 23 Nov 2009; published 30 Nov 2009

19. Y. N. Yang, B. Yang, J. R. Zhu, Z. H. Shen, J. Lu, and X. W. Ni, "Theoretical analysis and numerical simulation of the impulse delivering from laser-produced plasma to solid target," Chin. Phys. B **17**(4), 1318–1325 (2008).
20. J. D. Achenbach, *Wave propagation in elastic solids* (Elsevier, Amsterdam, 1975).

1. Introduction

Ultrasound can be generated by lasers and remotely detected by measuring a material's surface displacement with laser interferometers [1–4]. Laser-generated ultrasound is just one of the many optodynamic phenomena [5–7] that include all kinds of macroscopic motion which can be initiated by high-intensity laser light. In some cases [5,8,9] it is necessary to follow these high-frequency and high-amplitude displacements when they are superimposed on the low-frequency or even translatory motion of the measured object.

A typical example of optodynamics is the motion of a laser-propelled rod that moves in a step-like fashion until its motion ceases due to friction [10]. Recently, studies of the linear momentum transfer from a laser-induced ultrasonic wave to a rod [5] called for a contactless, preferably interferometric, method that enables measurements of laser-generated ultrasonic waves on moving objects. These high-frequency displacements have to be measured with nanometer resolution and the interferometer must be able to follow the motion of the object along its path for several hundred micrometers.

In general, displacement-measuring interferometers [11] can be divided into three main categories, based on their measurement range and resolution. Displacements that are several orders of magnitude longer than the wavelength of an interferometric laser are usually determined by counting the interference fringes, which is a low-resolution technique [1] appropriate for measuring linear motion. On the other hand, displacements that are small compared to the wavelength are usually measured around the most sensitive point of the detected signal. A typical representative of this category is the arm-compensated Michelson interferometer [5], which has a typical resolution of about 0.1 nm and a maximum displacement of ~100 nm, covering a dynamic range of 10^3. However, only low-amplitude ultrasonic waves (< 100 nm) can be measured with this type of interferometer. Interferometers in the third category can be represented by the homodyne quadrature laser interferometer (HQLI) [12], which combines the long measurement range and the high resolution. It is an interferometer with a constant sensitivity, which enables measurements of high-amplitude ultrasonic waves (> 100 nm) as well as the monitoring of ultrasonic waves superimposed on translatory moving objects.

The main aim of this paper is a qualitative demonstration of the nature of elastic-body motion. We performed a single-shot measurement on a laser-propelled rod with a HQLI over the entire period of its motion. In addition, this also provides a quantitative demonstration that the HQLI is an appropriate tool for measurements of high-amplitude ultrasonic waves (~1.3 μm) propagating and reverberating within a rod that slips on a frictional grounding by ~220 μm. Furthermore, the low-amplitude vibrations of the rod (~4 nm) can be detected once the rod has already been halted by the friction.

2. Experimental Setup

The ultrasonic waves on static objects can be monitored with different surface-displacement measuring methods, most commonly with piezoelectric transducers [13], capacitive sensors [14], electromagnetic acoustic transducers [15], and interferometers [1,5,12]. However, due to the contact nature of piezoelectric transducers, their application is limited, because of their influence on the boundary conditions and their low damage threshold. On the other hand, capacitive sensors and electromagnetic transducers have to be kept relatively close to the measuring surface, which makes these techniques inappropriate when the body motion has to be followed. Therefore, only interferometers that combine a long measurement range and a high resolution can be used to monitor the ultrasound on moving objects.

Our experimental setup, depicted in Fig. 1, is based on a HQLI that enables contactless measurements of high-amplitude ultrasound on moving objects in the frequency range DC to 200 MHz and a displacement range of 1 mm, and with a constant sensitivity below 1 nm.

#119489 - $15.00 USD Received 3 Nov 2009; accepted 23 Nov 2009; published 30 Nov 2009

Only a brief overview of the HQLI's operation will be given here, since a detailed description can be found in Ref [12].

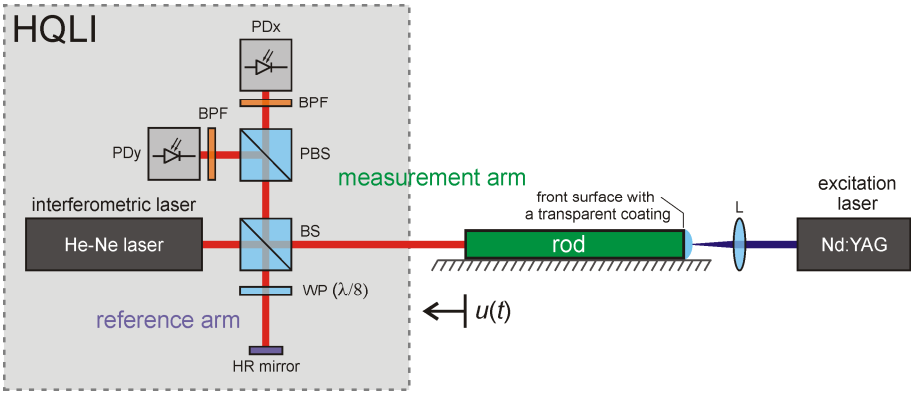

Fig. 1. Schematic diagram of the experimental setup. The front end of the rod is illuminated by a single Nd:YAG pulse. The axial displacement of rod's rear end is measured with the HQLI.

The HQLI is based on the detection of two orthogonally polarized beams with a 90° phase shift. The output beam from the laser is evenly split by a beam-splitter (BS) into the measurement and reference arms. The quadrature of both signals is achieved by a retardation plate (WP) in combination with the linearly polarized laser output and the polarization beam splitter (PBS). The signals from both photodiodes (PDx and PDy) were acquired and processed with specially developed software in order to obtain the desired displacement $u(t)$, which is encoded in the phase that accounts for the optical phase difference between the two arms arising from the displacement of the measuring surface. Optical band-pass filters (BPFs) were placed in front of both photodiodes in order to eliminate the scattered light from the excitation laser and the light emission of the laser-induced plasma. In contrast to an arm-compensated Michelson interferometer [5], which loses linearity and sensitivity when the measured displacement exceeds $\lambda/8$, the HQLI has a constant sensitivity and a high dynamic range of about 10^6.

A continuous He-Ne-type laser with an output power of 10 mW at 632.8 nm was applied as the interferometric laser. Its beam was reflected from the rear surface of the L = 120-mm-long steel (AISI: 304) rod with a radius of 1 mm. The front and rear surfaces of the rod were both cut straight and mirror-polished. The rod was placed on a flat aluminum grounding, so forming a frictional contact. The laser-induced motion of the rod was initiated by strong irradiation of its front surface, causing a confined material ablation. The excitation laser (Q-switched Nd:YAG, λ = 1064 nm) with 10-ns-long pulses and an energy of 300 mJ per pulse was focused on a 0.1-mm-diameter spot at the center of the front surface by a convergent lens (L). The illuminated surface was covered with transparent coatings (water and nail varnish) in order to increase the normal pressure [16], which enhances the linear momentum transfer and consequently increases the amplitude of the initial mechanical compression. In such a way, high-amplitude ultrasound was generated in order to demonstrate the capability of the HQLI for measurements of high-amplitude ultrasound on moving objects.

The signals from 200-MHz photodiodes were equidistantly sampled by a 500-MHz oscilloscope with a sampling capacity of 2 MS per channel. We made a single-shot measurement of the axial displacement of the rod's rear surface from the time when the excitation laser hit the rod's front surface to the end of the rod's motion.

3. Laser-induced motion

The motion of the laser-propelled rod, presented in Fig. 2, was monitored at its rear surface with the HQLI. Figure 2 shows two single-shot measurements with two different transparent coatings applied to the (illuminated) front surface of the rod. All the other experimental parameters were kept the same. Due to a different linear-momentum transfer, the total

#119489 - $15.00 USD Received 3 Nov 2009; accepted 23 Nov 2009; published 30 Nov 2009

displacement of the rod covered with nail varnish (the red curve) was smaller than the case when the front end was covered with water (the blue curve).

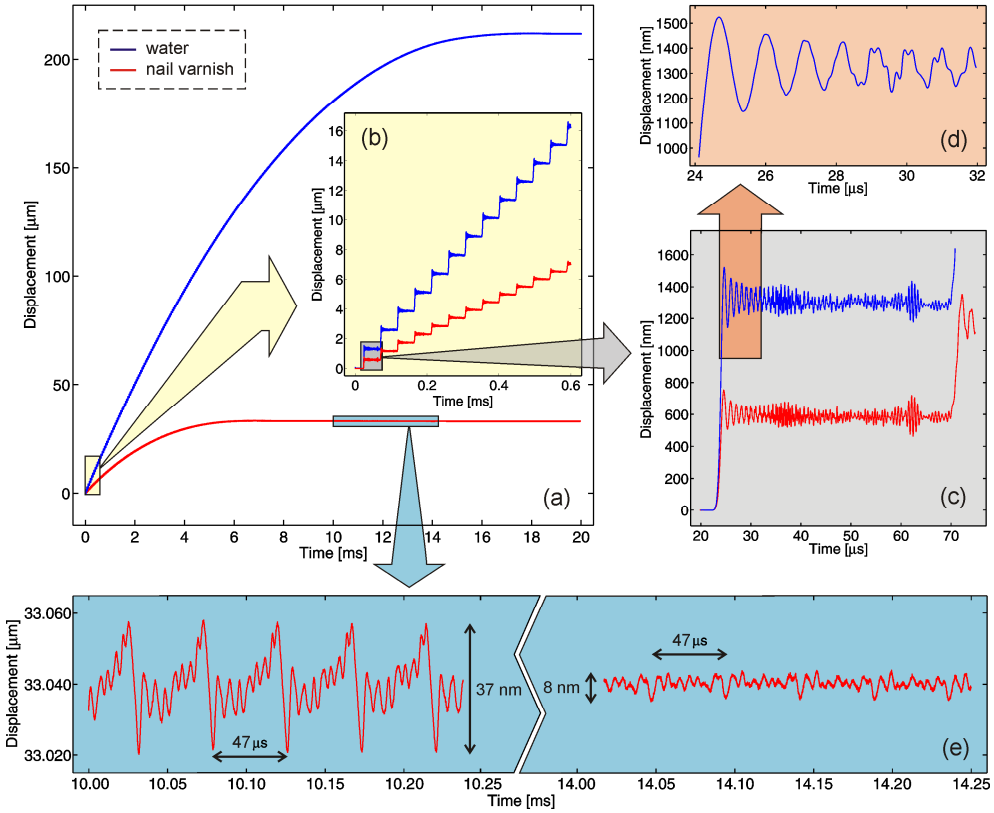

Fig. 2. The motion of a laser-ablated rod that moves in a step-like fashion until it stops due to friction. The axial displacement is measured in a single shot with the HQLI at the rear end of the L = 120-mm-long steel rod as a function of time. (a) The entire motion of the rod's rear end for the smaller (the red curve) and the higher (the blue curve) linear momentum transfer. (b) Magnification of the displacement shows that the rear end moves in abrupt discrete steps that are superimposed on a uniform motion. (c) Magnification of the first step. The high-frequency oscillations caused by the wave's geometrical dispersion are clearly seen. (d) Magnification of the first few oscillations inside the first step. The arrivals of the higher Pochhammer-Chree modes can be seen as a few MHz oscillations superimposed on the dominant frequency. (e) When the slippage ceases, the ultrasonic wave still rebounds from both rod terminations with a period of 47 µs, corresponding to twice the time-of-flight. The amplitude of the ultrasound decreases over time.

When the propelled rod is considered to be a rigid body or when its motion is measured with a low-resolution technique, the classical quadratic dependence of the displacement on the time of such motion is obtained:

$$v^*(t) = \begin{cases} v_0^*\left(1 - t/t_f\right); & 0 \le t \le t_f \\ 0; & t > t_f \end{cases} \quad \text{and} \quad u^*(t) = \begin{cases} v_0^* t\left(1 - t/(2t_f)\right); & 0 \le t \le t_f \\ v_0^* t_f/2; & t > t_f \end{cases}. \quad (1)$$

Here, v^* and u^* are the velocity and displacement of the rod's center of mass, respectively. The initial velocity is v_0^*, t is the time, and t_f is the time needed to reach the total displacement $u_\infty^* = v_0^* t_f/2$. This dependence is visible in our measurements in Fig. 2(a). Here, the high-resolution details are not visible due to the technical limitations of the printing. The general quadratic motion complies with the motion of the rod's center of mass, which has a

#119489 - $15.00 USD Received 3 Nov 2009; accepted 23 Nov 2009; published 30 Nov 2009

constant deceleration $a^* = v_0^*/t_f$ due to the frictional forces between the rod and the grounding in contact. Fitting the displacement (Eq. (1)) to the measured data in Fig. 2(a), using the least-squares method, we obtained the fitting parameters (v_0^*, t_f), which equal 3 mm/s and 16 ms for the blue curve, and 1 mm/s and 5 ms for the red curve. From these values we calculated a deceleration of ~2 m/s^2, which leads to a coefficient for the kinetic Coulomb dry friction of about 0.2.

However, a high-resolution device, such as the HQLI, has to be employed to demonstrate the richness of the nature of elastic-body motion that reveals the following details. The laser-induced motion of an elastic rod originates from the linear momentum transfer occurring during the light-material interaction. When the intensity of the laser pulse is high enough to surpass the material's ablation threshold, this interaction yields a pressure impulse that is exerted on the rod's surface. This pressure induces a mechanical wave within the rod near the interaction site. The acquired linear momentum is initially localized solely inside the mechanical compression (ultrasonic wave), which propagates along the rod with the thin-rod velocity c_0 and experiences numerous rebounds from both ends.

The nature of the interaction between the laser pulse and the material is visible in Fig. 2(b), which is a magnification of the first 600 μs of Fig. 2(a). Here, the motion immediately after the laser pulse is restricted to the mechanical wave. This wave is much shorter compared to the length of the rod L. After the time-of-flight $t_L = L/c_0 = 23.5$ μs—the time needed for the wave to reach the other end of the rod—the reflection of the mechanical wave causes a displacement of the rear end of the rod. However, after the reflection the end cross-section does not return to the initial position. This happens on every return n of the wave to the rear end at times $t = (1 + 2n)t_L$, leading to the discrete steps superimposed on a uniform motion. Figure 2(b) reveals that the mechanical wave, which is concealed in the elastic body, is responsible for its motion. The motion takes place only within the mechanical wave; the other parts of the rod are at rest. This is very clearly seen in the first few steps (a few hundred μs) when the influence of the friction and dispersion is sufficiently small.

Later on, the dispersion widens the initially short wave until the wave's length becomes comparable to the length of the rod. This is one of the mechanisms of the linear momentum transfer from the mechanical wave to the whole body. During the gradual stoppage of the rod due to friction the following interesting effect on the wave motion is observed at its rear end. Initially, the rod's rear end moves discretely only forward. Between successive wave reflections the rear end does not experience an average displacement. Later on, the rear end experiences an average backward displacement between successive reflections. This causes the flat steps to become more and more triangular with time.

To discern the step-like longitudinal motion of the elastic rod from the average motion of its rigid-body behavior, the generation time of the mechanical compression has to be much smaller than the time-of-flight. Mechanically generated transient ultrasonic pulses are usually ~100 μs long [17], while short-laser-pulse-induced ones last about as long as the duration of the laser pulse [18,19]. Compared to our 10-ns ones, even shorter laser pulses (in the ps and fs ranges) would not yield any significant change in the motion of the rod's rear end, since the effects of geometrical dispersion [8] broaden the width of the initial mechanical compaction (~10 ns) to about the same size (~1 μs), already in the first transit from the front to the rear end of our 120-mm rod.

The laser-induced mechanical wave is a short compression/rarefaction; therefore, it is comprised of high-frequency components. The Fourier components of different frequencies travel with different phase velocities according to the dispersion relations [8]. The effects of the geometric dispersion add a tail of alternating particle velocities to the wave's front. At the first arrival to the rear end, the wave's front is 1 μs wide and displaces the rod's rear end by the height (1.3 μm for the blue curve and 0.6 μm for the red curve) of a step [Fig. 2(c)]. The vibrating motion of the rear end in the time interval between 23.5 μs and 35 μs is caused by the lateral inertia [8]. The proceeding subtle displacements around the general step height before the arrival of the next wave correspond to the rich structure of the Pochhammer-Chree

#119489 - $15.00 USD Received 3 Nov 2009; accepted 23 Nov 2009; published 30 Nov 2009

(PC) dispersion relations for the axisymmetric, longitudinal, time-harmonic waves in an infinite rod [20]. Figure 2(d), which is a magnification of the time interval between 24 μs and 32 μs of Fig. 2(c), shows the arrival of the second PC mode, which is visible from 29 μs on as a few MHz oscillations superposed on the dominant carrier frequency.

Figure 2(e) is a magnification of the red curve in the time interval between 10 ms and 14 ms of Fig. 2(a) and shows the displacement of the rear end when the center of mass comes to rest, i.e., the total displacement is achieved. It can be seen that the rod is still vibrating with a double time-of-flight period of 47 μs, which is equal to the period of the fundamental normal mode of a free-free rod. The amplitude of vibrations around the stationary center of mass decreases (from 17.5 nm at 10 ms to 4 nm at 14 ms). The deceleration of the rod due to the acoustic emission is negligible compared to the transfer of the linear momentum to the clamping by frictional forces.

4. Conclusion

We have demonstrated the applicability of the HQLI for measurements of high-amplitude and high-frequency ultrasonic waves on moving objects. This demonstration was performed on an interesting example of laser-induced motion. Here, a single-shot displacement measurement of a laser-propelled rod's rear end was performed during the entire time of its motion. We reported on the first experimental demonstration of a laser-propelled, elastic-body motion where all the significant physical mechanisms that reveal the nature of its motion are seen from a single-shot measurement. With this measurement we showed the following: how the linear momentum is obtained by the rod in the form of a short mechanical wave; how the linear momentum of this wave is transferred to the whole body due to dispersion; and how the rod comes to rest because friction acts as a sink for the rod's linear momentum. A short explanation of these mechanisms was also provided.

#119489 - $15.00 USD Received 3 Nov 2009; accepted 23 Nov 2009; published 30 Nov 2009